This article has been accepted for publication in a future issue of this journal, but has not been fully edited. Content may change prior to final publication. Citation information: DOI 10.1109/TPEL.2019.2893238, IEEE Transactions on Power Electronics

Pressureless Silver Sintering on Nickel for Power Module Packaging

Meiyu Wang, Yunhui Mei*, *Member, IEEE*, Xin Li, Rolando Burgos, *Member, IEEE*, Dushan Boroyevich, *Life Fellow, IEEE*, and Guo-Quan Lu, *Fellow, IEEE*

***Abstract*-** Die-attach by low-temperature silver sintering has been widely used in power electronics packaging. Most of the reported work was done on direct-bond-copper (DBC) substrates metallized with silver or gold. There is a lack of studies of sintered-silver bonding on nickel (Ni), a low-cost metallization on DBC. In this study, we fabricated a power module using pressureless in-air sintered-silver die-attach on Ni-plated DBC substrate. Strong die-shear strength of over 40 MPa was achieved. It was also found the static and switching characteristics, the transient and steady-state thermal performance of the modules using Ni metallization was as good as that using Au metallization. Cross-sectional microstructure and chemistry analyses of the sintered-Ag/Ni interface revealed limited Ni oxidation. We believed that the high-density packing of silver particles and outgassing of the organic molecules from the paste during the bonding process helped to lower the partial pressure of oxygen in the bondline, which in turn, prevented rapid Ni oxidation and gave rise to extensive formation of strong Ag-Ni metallic bonds at the interface. The findings of this study show the low-cost potential of the die-attach technology for power module packaging since the bonding process can be done pressureless in air on low-cost Ni metallization.

***Keywords*-** pressureless silver sintering; Ni plating; die attach; power module

I. Introduction

The wide-band-gap (WBG) power devices (e.g. SiC and GaN) that can work at high power, frequency, and temperature, are increasingly used in numerous electronic applications, such as automotive, aircraft, and space exploration etc. In order to assure the high performance and reliability of the WBG power modules, all the packaging components have to be suited to more severe thermal and electrical constraints [1]. Among which, die-attachment of power devices to metallized substrates is a critical component in the power module packaging, since it greatly impacts the thermal, electrical, and reliability performance [1, 2]. Recently, low-temperature silver sintering was emerged to meet the demand for die-attachment in the WBG power modules, thanks to its high thermal, electrical, and reliability performance [3-7]. Most of the reported sintered-silver die-attachment have been done on bonding to direct-bond-copper (DBC) substrates that are metallized with noble metals such as silver(Ag) or gold(Au). Excellent sintered-silver bonding quality can be achieved on Ag or Au metallization in air for power module packaging [1-6].

Compared with Ag and Au, nickel (Ni) is another common metallization with much lower cost, which is widely used as a diffusion barrier interlayer or adhesion layer for DBC substrate, especially in aerospace applications [8]. Because Ni has low diffusion rate and reaction rate, the reliability could be enhanced without concerning the issue of electromigration and intermetallic compounds formation. Therefore, it will be significant to reduce the cost by die-attaching with Ni finish directly using the sintered silver. However, there is a lack of report of the strong sintered-silver bonding on Ni substrate so far. For die-attachment area of ~20 mm^2 on Ni substrate, Ogura *et al.* [9] obtained shear strength of 20 MPa when sintered at 300°C for 5 min in air under pressure of 5 MPa; Ishizaki *et. al.* [10] obtained shear strength of 15 MPa when sintered at 300°C for 5 min in hydrogen without pressure. It is very difficult to achieve strong sintered-silver bonds on Ni due to the inherent nature of Ni oxidation once upon exposure to air at high temperatures. The bonding strength will be weakened as the oxide hinders the atomic diffusion and metallic bonds at the bonding interface [11]. Therefore, in order to obtain strong sintered-silver bonding, Ni oxidation has to be prevented during sintering.

In this study, we fabricated a power module using pressureless in-air sintered-silver die-attach on Ni-plated DBC substrate. A high solid-loading (> 88wt.%) hybrid-silver paste was used, which is a uniform mixture of nano- and micro-scale silver particles in an organic solvent-surfactant system. It was found that the close packing of silver particles and outgassing of the organic molecules in the paste could prevent Ni from extensive oxidation, resulting in strong bonding strength at the Ag/Ni interface. Strong die-shear strength in excess of 40 MPa was achieved. It was also found the static and switching characteristics, and transient and steady-state thermal performance of the modules using Ni metallization to be as good as that using Au metallization. The findings of this study showed the low-cost potential of the die-attach technology for power module packaging since the bonding process can be done pressureless in air on low-cost Ni metallization.

Meiyu Wang, Yunhui Mei, and Xin Li are with the Key Laboratory of Advanced Ceramics and Machining Technology of Ministry of Education, and School of Materials Science and Engineering, Tianjin University, Tianjin, 300350, China (email: meiyuwang@tju.edu.cn, yunhui@tju.edu.cn, xinli@tju.edu.cn). Dr. Yunhui Mei is the corresponding author of this work.

Rolando Burgos and Dushan Boroyevich are with the Center for Power Electronics Systems (CPES), Bradley Department of Electrical and Computer Engineering, Virginia Tech, Blacksburg, VA 24061, USA (email: rolando@vt.edu, dushan@vt.edu)

Guo-Quan Lu is with the Center for Power Electronics Systems (CPES), Bradley Department of Electrical and Computer Engineering, and Department of Materials Science and Engineering, Virginia Tech, Blacksburg, VA 24061, USA (email: gqlu@vt.edu)

This article has been accepted for publication in a future issue of this journal, but has not been fully edited. Content may change prior to final publication. Citation information: DOI 10.1109/TPEL.2019.2893238, IEEE Transactions on Power Electronics

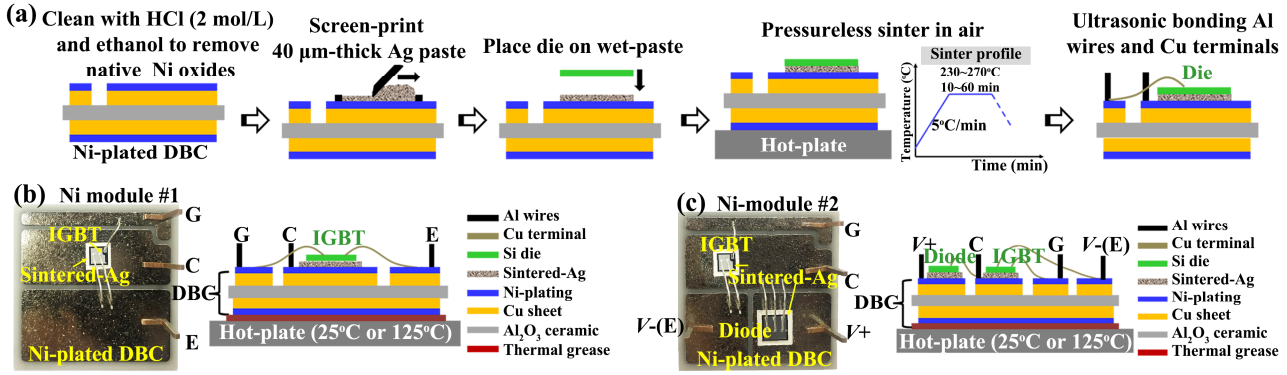

Fig. 1 (a) Ni-Module fabrication process, (b) Ni-module fabricated for microstructural, mechanical, thermal, and static output characteristics tests, and (c) Ni-module fabricated for switching characteristics test.

II. Modules Fabrication

Fig. 1 shows the module fabrication process. The modules were fabricated by attaching silver-plated silicon IGBT devices (Infineon, IGC15T65QE, 650 V, 30 A, 3.92×3.88×0.07 mm^3) on Ni(P) electroless-plated DBC substrates (Curamik Rogers) using a hybrid-silver paste sintered in air without pressure. For comparison, the same die-attachment on Au electroless-plated DBC substrates (Curamik Rogers) were sintered and tested under the same conditions as well. At least five modules for each test condition below were fabricated. To facilitate description, the modules using Ni-plated DBC and Au-plated DBC are named as Ni-module and Au-module hereinafter, respectively. With proper selection of organic chemistry, the paste has good flow characteristics for screen printing at a solid loading of over 88wt.%. The paste is a trimodal system, by mixing nano-scale (62 nm), submicron-scale (0.4 μm), and micro-scale (2.5 μm) silver particles with volume percent of 3.5%, 35.5%, and 61%, respectively. It was reported that in the absence of pressure during sintering, the packing density alone could reach 65%, 87% and 95% for mono, bimodal and trimodal systems of silver particles, respectively [2, 12]. Thanks to its higher initial packing density, the trimodal system silver paste can achieve higher bonding strength than bimodal or mono system silver paste [2].

III. Results and Discussion

A. Microstructure analysis

To understand the bonding mechanisms between sintered-Ag and Ni, we analyzed the fracture surface and cross-sectional microstructures and chemistries of the sintered bondline by scanning electron microscopy (SEM), energy dispersive spectrometer (EDS), and electron probe micro-analyzer (EPMA), respectively. As shown in Fig. 2(a), the fracture surface on Ni-plating exhibits a cohesive failure, which usually demonstrates a strong bonding. The de-bonding occurs mostly within sintered-Ag bondline (location A) and partly at sintered-Ag/Ni interface (location B), indicating a strong interfacial bonding between sintered-Ag and Ni-plating. The dispersive sintered-Ag residuals are also observed at location B on the Ni-plating. From the SEM image of the cross-sectional bondline as shown in Fig. 2(b), we can see that the sintered-Ag bonds well with the Ni-plating with neither delamination nor de-bonding. The EPMA line scan result in Fig. 2(c) shows a well-defined sintered-Ag/Ni interface, suggesting no intermetallic formation and low inter-diffusion rate between Ag and Ni. No evidence of oxygen at the interface is found, indicating effective prevention of Ni oxidation by outgassing of organic molecules from paste during sintering. Extensive formation of metallic bonds between sintered Ag and Ni is the most likely reason leading to strong bonding and excellent electrical and thermal performance.

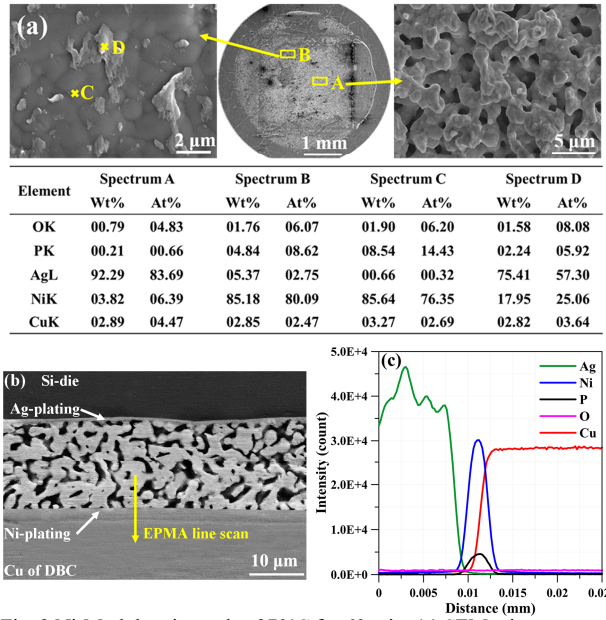

Element	Spectrum A		Spectrum B		Spectrum C		Spectrum D	
	Wt%	At%	Wt%	At%	Wt%	At%	Wt%	At%
OK	00.79	04.83	01.76	06.07	01.90	06.20	01.58	08.08
PK	00.21	00.66	04.84	08.62	08.54	14.43	02.24	05.92
AgL	92.29	83.69	05.37	02.75	00.66	00.32	75.41	57.30
NiK	03.82	06.39	85.18	80.09	85.64	76.35	17.95	25.06
CuK	02.89	04.47	02.85	02.47	03.27	02.69	02.82	03.64

Fig. 2 Ni-Modules sintered at 270°C for 60 min: (a) SEM microstructure and EDS composition images taken from fracture surface after die-shear test, (b) cross-sectional SEM microstructure image, and (c) cross-sectional EPMA composition line scan result.

B. Mechanical characteristics

The mechanical performance of the sintered-Ag joints was evaluated by die-shear strength (Dage 4000 bond-tester). As shown in Fig. 3(a), the shear strengths increase with higher sintering temperature or longer sintering time. The reason is that both the cohesive strength from sintered bondline densification and adhesive strength at bonding interfaces from metallic bonds and atomic motion are enhanced at higher sintering temperature or over longer sintering time [11]. When sintered at 230°C, the die-shear strengths on both of the Ni and Au are only about 10 MPa, due to non-densification sintering at low temperature. When sintered at 240°C, the shear strength on Au is in excess of 30 MPa, while that on Ni is only around 15 MPa. This disparity could be ascribed to the disparate interdiffusivity between Ag/Au and Ag/Ni. It is reported that the diffusivity of Ag in Au is 10000 times higher than that of Ag in Ni [11]. When sintered at 270°C, the shear strengths of all die-attachments are in excess of 40 MPa. The strong bonding

This article has been accepted for publication in a future issue of this journal, but has not been fully edited. Content may change prior to final publication. Citation information: DOI 10.1109/TPEL.2019.2893238, IEEE Transactions on Power Electronics

could be attributed to both the strong cohesive strength and adhesive strength, resulting from high solid loading and high packing density of the trimodal hybrid-silver paste, and Ni oxidation prevention by outgassing organics in the paste during sintering.

C. Static characteristics

The static output I-V characteristics of the modules were tested at V_{GE}=15V using Agilent B1505A power device analyzer curve tracer. The modules were tested at 25℃ or 125℃ by adjusting the hotplate temperature underneath the modules (schema shown in Fig. 1(b)). As seen in Fig. 3(d), when tested at 125℃ rather than 25℃, all the I-V curves shift to the right, showing a monotonously increasing R_{on} by approximately 8%. The slope of the output I-V curve keeps increasing with higher sintering temperature, evidencing improved electrical conductivity of sintered bondline at the higher temperature. The measured static characteristics are consistent with the die-shear strength. That is, the $V_{CE(sat)}$ of the modules sintered at 230℃ are ~6% higher than that sintered at ≥250℃, due to high resistance from non-densification sintered bondline at 230℃. The disparity of $V_{CE(sat)}$ is small (<2%) between all modules sintered ≥250℃. The measured static characteristics of Ni-modules are as good as that of Au-modules, i.e. disparity of 1% (except 3% disparity of modules sintered at 240℃), indicating excellent electrical conductivity of sintered-Ag die-attach on Ni-plated substrates.

D. Switching characteristics

The switching characteristics were measured using the standard double-pulse testing method [5, 13]. In the module under test as shown in Fig. 1(c) and Fig. 3(c), a 1200-V, 50-A silicon diode (Infineon, SIDC30D120H8, 5.5×5.5×0.12 mm^3) was used as the freewheeling diode. The switching tests were conducted under 300 V and 30 A at 25℃ or 125℃. As shown in Fig. 3 (c), when tested at 125℃ rather than at 25℃, the I_C and V_{CE} waveforms show a right shift, indicating a longer turn-on and turn-off delay time and a slower *di/dt* and *dv/dt* in the I_C and V_{CE} waveforms [14]. As shown in Fig. 3(d), the switching time and loss tested at 125℃ is ~10% higher than that tested at 25℃. It is reported that the IGBT turn-on loss is increased at higher temperature mainly due to the increased diode reverse recovery current, while the prolonged minority carrier lifetime slows down the IGBT turn-off speed and increases the turn-off loss [14]. The increased switching time and loss should be related to the temperature-dependent characteristics of IGBT and diode devices, which are not determined by the die-attachment. It seems that the electrical conductivity of die-attachment has little influence on the switching characteristics. The switching on/off time and loss of modules sintered at different temperatures (230℃-270℃) almost keep constant (disparity within 2%). The double pulse test was done to verify that the devices attached on the Ni-plating could be switched functionally. The devices were not degraded during the die-attach process. The switching characteristics of Ni-modules were consistent with that of Au-modules (variation within 2%), which was proved as a robust Ag-Au die-attachment [2, 3], confirming the feasibility of attaching the power devices with Ni-plating surface by silver sintering.

E. Transient thermal characteristics

The transient thermal performance of the modules was evaluated by transient thermal impedance Z_{th} (self-made tester [15]). The Z_{th} was measured electrically using V_{GE} as temperature sensitive parameter, and calculated as follows [15]:

$$Z_{th} = \frac{\Delta T_J}{P_H} = \frac{\Delta V_{GE}}{K \times P_H} \quad (1)$$

where P_H (50 W) is the power dissipation, and K (10.3 mV/℃) is the coefficient of V_{GE} with respect to T_J. Fig. 4(a) shows the schematic waveforms and heat conduction time within the module. Based on thermal diffusion theory, the heat just conducts within the module at heating time t_H less than total heat conduction time τ. Therefore, the Z_{th} was measured at t_H≤25 ms (τ=26.42 ms as shown in Fig.4 (a)). As seen in Fig. 4(b), the Z_{th} increases with t_H, as heat conducts through more layers with longer heating time. Overall, the Z_{th} decreases with higher sintering temperature, evidencing improved thermal conductivity of sintered-Ag bondline. Quite consistent with the measured static output characteristics, the Z_{th} of all the Ni- and Au-modules sintered at 230℃ are ~6% higher than that of the modules sintered at ≥250℃, due to the lower thermal conductivity of non-densification sintered bondline at 230℃. The Z_{th} of Ni-modules sintered at 240℃ is ~3% higher than that of Au-modules, because of higher interface thermal resistance from weaker adhesion at sintered-Ag/Ni interface. When sintered at ≥250℃, all the Z_{th} curves almost overlap together, revealing insignificant improvement of thermal performance with higher sintering temperature. The measured Z_{th} of Ni-modules (except that sintered at 240℃) has high consistency with that of Au-modules, indicating the excellent transient thermal performance of sintered-Ag die-attach on Ni-plated substrates.

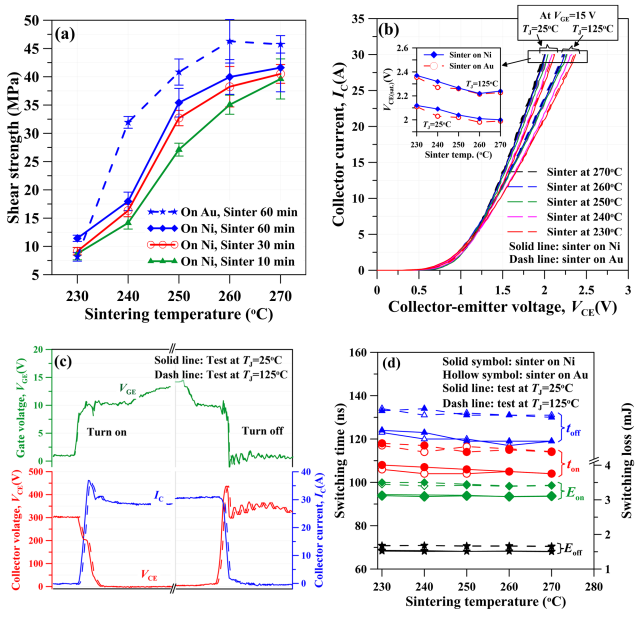

Fig. 3 (a) die-shear strength, (b) static output characteristics, (c) switching waveforms, and (d) switching time and loss results of Ni-modules and Au-modules sintered at 230℃-270℃ for 60 min. (Note: the symbols or lines are averaged data of five tested samples, and the error bars are samples standard deviation.)

F. Steady-state thermal characteristics

The steady-state thermal performance of the modules was evaluated by steady-state junction temperature (T_J) measured by infrared thermography. Fig. 4(c) and Fig. 4(d) show the test condition and measured steady-state T_J of modules versus

This article has been accepted for publication in a future issue of this journal, but has not been fully edited. Content may change prior to final publication. Citation information: DOI 10.1109/TPEL.2019.2893238, IEEE Transactions on Power Electronics

sintering temperature, respectively. Similar with Z_{th} results, the T_J measured at steady-state decreases with higher sintering temperature, evidencing improved steady-state thermal performance of sintered-Ag bondline. The Z_{th} of all modules sintered at 230°C is ~10% higher than that sintered at 270°C, due to the poorer thermal performance of non-densification sintered bondline at 230°C. Overall, T_J of the Ni-modules is slightly higher (<1.5%) than that of the Au-modules, except that sintered at 240°C with disparity of ~4%. The measured steady-state T_J of Ni-modules has high consistency with that of Au-modules, indicating the excellent steady-state thermal performance of sintered-Ag die-attach on Ni-plated substrates.

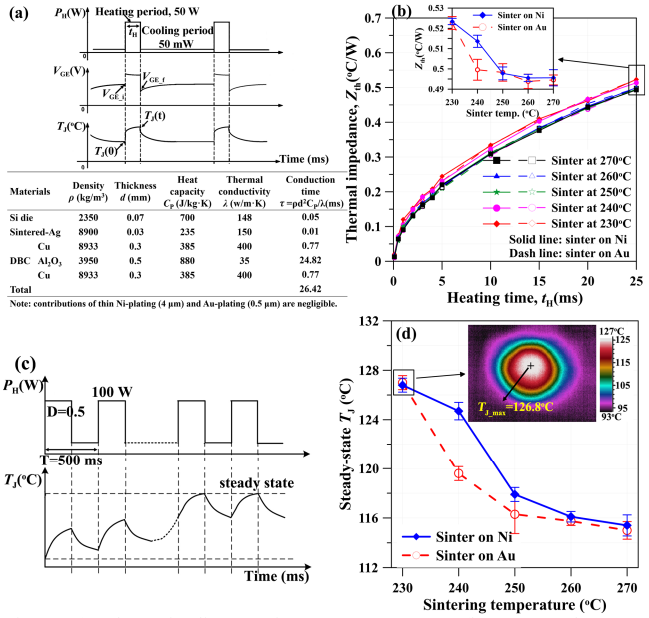

Fig. 4 (a) schematic diagram for Z_{th} measurement, (b) measured Z_{th}, (c) schematic diagram for steady-state T_J measurement, and (d) measured steady-state T_J results of Ni- and Au-modules sintered at 230°C-270°C for 60 min. (Note: the symbols or lines are averaged data of five tested samples, and the error bars are samples standard deviation.)

TABLE I. COMPARISON OF SILVER-SINTERING ON DIFFERENT SURFACE FINISHES.

Plating on DBC	Ni(5 μm)	Ni(5 μm) /Au(1 μm)	Ni(5 μm) /Ag(1 μm)
Cost of plating materials [16]	$0.015/g	$45/g	$0.5/g
Die-shear strength	20 MPa in [9]	30 MPa in [2, 3]	30 MPa in [2]
	41 MPa (in this work)	45 MPa (in this work)	/
Thermal impedance Z_{th}	0.496°C/W (in this work)	0.495°C/W (in this work)	0.57 °C/W in [17]
Parasitic inductance	24.13 nH	24.49 nH	25.53 nH
Parasitic resistance	1.287 mΩ	1.292 mΩ	1.299 mΩ

Table I shows the comparison of silver sintering on different surface finishes. The parasitic inductance and resistance were extracted using ANSYS Q3D of the power module geometry shown in Fig. 1 (b). For fixed cross section, to minimize the parasitic inductance, the length through which the current passes should be minimized [18]. By removing the Au or Ag plating, the parasitic inductance and resistance would decrease slightly since the loop length decreased. Compared with the power modules using Ni/Au-plating and Ni/Ag-plating, for the power module using Ni-plating, the parasitic inductance decreases by 1.5% and 5.8%, and the parasitic resistance decreases by 0.4% and 0.9%, respectively.

IV. CONCLUSIONS

In this study, a power module using pressureless in-air sintered-silver die-attach on Ni-plated DBC substrate was fabricated. Microstructural and chemical analyses of the cross-sectional bondline revealed limited Ni oxidation at the bonding interface. We believed that the high-density packing of hybrid-silver particles in the paste and outgassing of the organic molecules from the paste during the bonding process helped to lower the partial pressure of oxygen in the bondline, which in turn, prevented rapid oxidation of nickel and gave rise to extensive formation of strong Ag-Ni metallic bonds at the interface. Consequently, the strong die-shear strengths in excess of 40 MPa were obtained. It was also found the static and switching characteristics, the transient and steady-state thermal performance of the modules using Ni metallization to be as good as (disparity within 3%) that using Au metallization. The findings of this study showed the low-cost potential of the die-attach technology for power module packaging since the bonding process can be done pressure-less in air on low-cost nickel metallization.

ACKNOWLEDGMENTS

This work was supported by the Science Challenge Project (No. TZ2018003), the National Natural Science Foundation of China (No. 51877147), and the Tianjin Municipal Natural Science Foundation (No.17JCYBJC19200), the CPES Industry Partnership Program, and the DOE ARPA-E Project.

REFERENCES

[1] R. Khazaka, L. Mendizabal, and D. Henry, *et al.*, "Survey of high-temperature reliability of power electronics packaging components," *IEEE Transactions on Power Electronics,* vol. 30, no. 5, pp. 2456-2464, 2015.

[2] K. S. Siow and Y. Lin, "Identifying the development state of sintered silver (Ag) as a bonding material in the microelectronic packaging via a patent landscape study," *Journal of Electronic Packaging,* vol. 138, no. 2, p. 020804, 2016.

[3] F. Yu, J. Cui, and Z. Zhou, *et al.*, "Reliability of Ag sintering for power semiconductor die attach in high-temperature applications," *IEEE Transactions on Power Electronics,* vol. 32, no. 9, pp. 7083-7095, 2017.

[4] P. Ning, T. G. Lei, and F. Wang, *et al.*, "A novel high-temperature planar package for SiC multichip phase-leg power module," *IEEE Transactions on power Electronics,* vol. 25, no. 8, pp. 2059-2067, 2010.

[5] S. Fu, Y. Mei, and X. Li, *et al.*, "Reliability evaluation of multichip phase-leg IGBT modules using pressureless sintering of nanosilver paste by power cycling tests," *IEEE Transactions on Power Electronics,* vol. 32, no. 8, pp. 6049-6058, 2017.

[6] L. A. Navarro, X. Perpina, and P. Godignon, *et al.*, "Thermomechanical assessment of die-attach materials for wide bandgap semiconductor devices and harsh environment applications," *IEEE transactions on Power Electronics,* vol. 29, no. 5, pp. 2261-2271, 2014.

[7] P. Ning, R. Lai, and D. Huff, *et al.*, "SiC wirebond multichip phase-leg module packaging design and testing for harsh environment," *IEEE Transactions on Power Electronics,* vol. 25, no. 1, pp. 16-23, 2010.

[8] J. G. Bai, J. N. Calata, and G. Lei, *et al.*, "Thermomechanical reliability of low-temperature sintered silver die-attachment," in *Thermal and Thermomechanical Phenomena in Electronics Systems, 2006. ITHERM'06. The Tenth Intersociety Conference on*, 2006, pp. 1126-1130: IEEE.

[9] T. Ogura, S. Takata, and M. Takahashi, *et al.*, "Effects of reducing solvent on copper, nickel, and aluminum joining using silver nanoparticles derived from a silver oxide paste," *Materials transactions,* vol. 56, no. 7, pp. 1030-1036, 2015.

[10] T. Ishizaki, K. Akedo, and T. Satoh, *et al.*, "Pressure-free bonding of metallic plates with Ni affinity layers using Cu nanoparticles," *Journal of Electronic Materials,* vol. 43, no. 3, pp. 774-779, 2014.

[11] G.-Q. Lu, M. Wang, and Y. Mei, *et al.*, "Advanced die-attach by metal-powder sintering: the science and practice," *CIPS 2018, 10th International Conference on Integrated Power Electronics Systems, VDE,* 2018.

[12] Y. Morisada, T. Nagaoka, and M. Fukusumi, *et al.*, "A low-temperature pressureless bonding process using a trimodal mixture system of Ag nanoparticles," *Journal of electronic materials,* vol. 40, no. 12, p. 2398, 2011.

[13] Z. Chen, Y. Yao, and D. Boroyevich, *et al.*, "A 1200-V, 60-A SiC MOSFET multichip phase-leg module for high-temperature, high-frequency applications," *IEEE Transactions on Power Electronics,* vol. 29, no. 5, pp. 2307-2320, 2014.

[14] Z. Xu, M. Li, and F. Wang, *et al.*, "Investigation of Si IGBT Operation at 200°C for traction applications," *IEEE Transactions on Power Electronics,* vol. 28, no. 5, pp. 2604-2615, 2013.

[15] M.-Y. Wang, G.-Q. Lu, and Y.-H. Mei, *et al.*, "Electrical method to measure the transient thermal impedance of insulated gate bipolar transistor module," *IET Power Electronics,* vol. 8, no. 6, pp. 1009-1016, 2015.

[16] H. Sverdrup, D. Koca, and K. V. Ragnarsdottir, "Investigating the sustainability of the global silver supply, reserves, stocks in society and market price using different approaches," *Resources, Conservation and Recycling*, vol. 83, pp. 121-140, 2014.

[17] X. Cao, T. Wang, and K. D. T. Ngo, *et al.*, "Characterization of lead-free solder and sintered nano-silver die-attach layers using thermal impedance," *IEEE Transactions on Components, Packaging and Manufacturing Technology*,vol. 1, no. 4, pp. 495-501, 2011.

[18] T. Meade, D. O. Sullivan, and R. Foley, *et al.*, "Parasitic inductance effect on switching losses for a high frequency DC-DC converter," *IEEE*, 2008.